Number fluctuation spectra from light scattered by particles in Brownian motion

1976 J. Phys. A: Math. Gen. 9 561

(http://iopscience.iop.org/0305-4470/9/4/013)

J. Phys. A: Math. Gen., Vol. 9, No. 4, 1976. Printed in Great Britain.

Number fluctuation spectra from light scattered by particles in Brownian motion

Richard F Voss† and John Clarke

Department of Physics, University of California and Inorganic Materials Research Division, Lawrence Berkeley Laboratory, Berkeley, California 94720, USA

Received 12 August 1975, in final form 3 November 1975

Abstract. We show that the spectrum of intensity fluctuations of monochromatic light scattered by a suspension of particles undergoing Brownian motion contains a contribution, $S_N(f)$, due to fluctuations in the number of illuminated particles in addition to the interference terms. Limiting forms of $S_N(f)$ are given for a regular three-dimensional illuminated volume Ω_i. For an Ω_i with sharp boundaries $S_N(f) \rightarrow An_0D^{1/2}/2\pi^{3/2}f^{3/2}$ for $f \gg D/l^2$, where l is the smallest dimension of Ω_i, D is the diffusion constant, n_0 is the particle number density, and A is the surface area through which particles may enter or leave Ω_i. We have measured the intensity fluctuation spectra of laser light scattered by suspensions of polystyrene spheres in water from 5×10^{-4} Hz to 5×10^{3} Hz. The spectra clearly show the usual homodyne Lorentzian superimposed upon $S_N(f)$. The effects of varying D, n_0, Ω_i, and detector area on the spectra were in excellent agreement with theory. The measured $f^{-3/2}$ limit of $S_N(f)$ together with D (from the Lorentzian halfwidth) and our known Ω_i enabled us to determine a value for n_0. $S_N(f)$ was also measured with a white light source.

1. Introduction

The intensity fluctuations of monochromatic coherent light scattered by a suspension of independent particles undergoing Brownian motion have been used to measure the diffusion constant, D, of the particles (see Cummins and Swinney 1970 for an extensive review). Similar methods have also been used to gain information about the motion of motile organisms (Schaefer *et al* 1974). Two closely related experimental techniques have been developed, namely heterodyne and homodyne detection. In the heterodyne experiment, first performed by Cummins *et al* (1964), light scattered by the particles is mixed with light of constant phase from the same source, which acts as a local oscillator. Interference between the constant phase component and the light scattered by each independent particle gives rise to intensity fluctuations. The heterodyne spectrum is, therefore, proportional to $\langle N \rangle$, the average number of illuminated particles. In the homodyne experiment, first performed by Ford and Benedek (1965), only light scattered from the particles is detected. The intensity fluctuations arise from interference between the light scattered by pairs of particles: as one particle moves relative to another, the phase difference of their electric fields at the detector varies. The fluctuation spectrum is thus proportional to the number of pairs of illuminated particles, $\langle N \rangle^2$

† Present address: IBM Laboratories, Yorktown Heights, NY 10598, USA.

Both of these interference effects depend on the coherent nature of the incident light. The heterodyne and homodyne experiments may be considered as an elastic scattering of light from wavevector $\boldsymbol{k}$ to $\boldsymbol{k}'$ by $n_{\boldsymbol{K}}$, a density fluctuation of wavevector $\boldsymbol{K}=\boldsymbol{k}'-\boldsymbol{k}$. The autocorrelation function for the intensity then depends on the average manner in which $n_{\boldsymbol{K}}$ decays in time. For independent particles undergoing Brownian motion $\langle \delta n_{\boldsymbol{K}}(t)\rangle = \langle \delta n_{\boldsymbol{K}}(0)\rangle \exp(-DK^2 t)$. The fluctuations are thus correlated over a time $\tau_c \approx 1/DK^2$. By measuring τ_c or the shape of the spectrum, $S_i(f) \propto \tau_c/[1+(2\pi\tau_c f)^2]$, one is able to determine D.

More recently, Schaefer and Berne (1972) studied suspensions of polystyrene spheres in water when the average number of particles, $\langle N\rangle$, in the illuminated volume, Ω_i, was very small. In this limit, the relative fluctuations in the number of particles become significant, and introduce additional intensity fluctuations in the scattered light. These additional fluctuations are not an interference effect but arise because the intensity of the scattered light is sensitive to the number of particles in Ω_i. Number fluctuations have also been observed by the fluorescence of individual particles (Elson and Magde 1974, Magde *et al* 1974). The correlation time for the number fluctuations is of the order l^2/D, where l is the smallest dimension of Ω_i, and is usually much greater than $1/DK^2$. Schaefer and Berne showed that the number fluctuations may be observed as a slowly varying excess background in the homodyne autocorrelation function. They were able to subtract out the contribution of the number fluctuations, and thus recover the usual homodyne autocorrelation function. The statistics of the non-Gaussian scattered light were discussed by Schaefer and Pusey (1972) and by Pusey *et al* (1974). From these measurements, one is able to deduce a value for the particle number density, n_0.

In this paper we present an alternative approach to the problem. First, we derive the intensity fluctuation spectrum for the scattered light. In addition to the homodyne and heterodyne terms, the spectrum contains a number fluctuation term, $S_N(f)$. The calculation of the spectrum is independent of the statistics. In the high frequency limit ($f \gg D/l^2$) for an illuminated volume with surface area A and with sharp boundaries, we find $S_N(f) = n_0 D^{1/2} A/2\pi^{3/2} f^{3/2}$. Therefore, a measurement of the high frequency limit of $S_N(f)$ allows one to determine n_0 if A and D are known.

Second, we describe a series of homodyne experiments in which laser light was scattered by a suspension of polystyrene spheres in water. The spectra of the intensity fluctuations of the scattered light were measured from 5×10^{-4} Hz to 5×10^{3} Hz. The spectra show clearly both the homodyne Lorentzian and $S_N(f)$. In most cases, the two spectra can easily be separated. Spectra were also obtained with a white light source: in this case, the interference Lorentzian was absent, and only $S_N(f)$ was observed. This technique provides an extremely sensitive method for detecting number fluctuations. The fluctuations were readily observable when $\langle N\rangle = 5{\cdot}5\times10^4$ for an unstabilized laser and $\langle N\rangle = 8\times10^6$ for an incandescent bulb. The observed spectra are in excellent quantitative agreement with the theoretical predictions. To our knowledge, these observations represent the first detailed experimental confirmation of the theory of number fluctuations in diffusive systems by a direct measurement of the spectra.

2. Theory

Light of wavevector $\boldsymbol{k}$ illuminates a small subvolume Ω_i of a cell of total volume Ω containing a suspension of $M = n_0\Omega$ particles (where $M \gg 1$) undergoing Brownian

motion. We assume that each of the particles is independent, and that Ω is large enough that we may neglect effects due to its boundaries. Each of the illuminated particles scatters the light elastically with a phase that varies in time due to the motion of the particles. We are interested in the intensity fluctuation spectrum for light scattered with wavevector $\boldsymbol{k}'$ into a detector of area A_{det}. Initially, we assume that the light is coherent over the area of the detector. The electric field is of the form

$$\boldsymbol{E}(t) = \boldsymbol{E}_0 \exp(-i\omega_0 t) + \beta \sum_{j=1}^{M} B(\boldsymbol{r}_j) \exp(-i\omega_0 t) \exp(i\boldsymbol{K} \cdot \boldsymbol{r}_j). \tag{1}$$

$\boldsymbol{E}_0$ is the constant phase heterodyne component, and $\boldsymbol{K} = \boldsymbol{k}' - \boldsymbol{k}$ is the scattering vector. $B(\boldsymbol{r}_j) = 1$ if $\boldsymbol{r}_j$ is in Ω_i, while $B(\boldsymbol{r}_j) = 0$ otherwise. β^2 is proportional to the intensity of the light scattered by a single particle as measured by the detector. The intensity of the scattered light is $I(t) = \boldsymbol{E}(t) \cdot \boldsymbol{E}^*(t)$.

We assume further that $|\boldsymbol{K}| \gg l^{-1}$, where l is the smallest dimension of Ω_i. This assumption is equivalent to setting $B_{\boldsymbol{K}} = 0$, where

$$B_{\boldsymbol{q}} \equiv (2\pi)^{-1/2} \int_{\Omega} B(\boldsymbol{r}) \exp(i\boldsymbol{q} \cdot \boldsymbol{r}) \, d^3\boldsymbol{r}.$$

The positive frequency spectrum of the intensity fluctuations can then be calculated in a straightforward way: this calculation is sketched in the Appendix. For a homodyne experiment for which $\boldsymbol{E}_0 \to 0$, the relative spectrum is

$$\frac{S_I(f)}{\bar{I}^2} = \frac{8DK^2}{4D^2K^4 + (2\pi f)^2} + \frac{S_N(f)}{\langle N \rangle^2} \tag{2}$$

where

$$S_N(f) = 4n_0 D \int \frac{|B_q|^2 q^2 \, d^3\boldsymbol{q}}{D^2q^4 + (2\pi f)^2}, \tag{3}$$

$\bar{I}$ is the average intensity, and $\langle N \rangle = n_0\Omega$. The first term on the right-hand side of equation (2) is the homodyne Lorentzian (Cummins and Swinney 1970). $S_N(f)$ arises from the number fluctuations (van der Ziel 1954, see also van Vliet and Fasset 1965 for a comprehensive review).

Whereas the homodyne Lorentzian depends on the coherent nature of the light, $S_N(f)$, which is independent of $\boldsymbol{K}$, does not depend on coherence but rather on the shape of Ω_i. Except for a few special cases, it is impossible to give an analytic expression for $S_N(f)$. It is, however, possible to determine its general behaviour. For a regular volume with dimensions $l_1 \geqslant l_2 \geqslant l_3$, there are three characteristic frequencies, $f_j = D/\pi l_j^2$, that divide the spectrum into four regions:

$$\begin{aligned} &S_N(f) \propto \text{constant} && \text{for } f \ll f_1, \\ &S_N(f) \propto \ln(1/f) && \text{for } f_1 \ll f \ll f_2, \\ &S_N(f) \propto f^{-1/2} && \text{for } f_2 \ll f \ll f_3, \end{aligned} \tag{4}$$

and

$$S_N(f) \propto f^{-3/2} \qquad \text{for } f \gg f_3.$$

The characteristic frequencies correspond to the times τ_j required for a particle to diffuse across Ω_i in the different directions: $f_j^{-1} \propto \tau_j \propto l_j^2/D$. At high enough frequencies ($f \gg f_3$) particles do not have enough time to diffuse across Ω_i in any direction, and the

fluctuations are insensitive to the exact shape of Ω_i. Changes in the number of particles in Ω_i then arise only from local one-dimensional diffusion across each surface element. Since each surface element is independent, $S_N(f)$ is proportional to A, the total surface area through which particles may enter or leave Ω_i:

$$S_N(f) \to 4n_0 D \int \frac{|B'_q|^2 q^2 \, dq}{D^2 q^4 + (2\pi f)^2} \qquad (f \gg f_3). \tag{5}$$

$B'(x)$ is the shape of the boundary of Ω_i in a direction normal to the surface. B'_q is the one-dimensional spatial Fourier transform of $B'(x)$. For a sharp boundary, $B'(x)=1$ for $x \leqslant 0$ and $B'(x)=0$ otherwise. Thus $|B'_q|^2 = 1/2\pi q^2$ and

$$S_N(f) \to \frac{2n_0 DA}{\pi} \int \frac{dq}{D^2 q^4 + (2\pi f)^2} = \frac{n_0 D^{1/2} A}{2\pi^{3/2} f^{3/2}} \qquad (f \gg f_3). \tag{6}$$

The $f^{-3/2}$ behaviour is therefore a consequence of particle flow across a sharp boundary. If, instead, the boundary has a finite width, w (for example, $B'(x)=1$ for $x \leqslant 0$ and $B'(x)=e^{-x/w}$ for $x>0$), we find

$$S_N(f) \propto n_0 DA/wf^2, \qquad \text{for } f \gg D/\pi w^2. \tag{7}$$

The constant of proportionality depends on the explicit shape of the boundary.

Although we initially assumed that the scattered light was coherent over the area of the detector, A_{det}, this assumption is usually not valid experimentally. In most cases the coherence area at the detector, A_{coh}, is less than A_{det}. Cummins and Swinney (1970) show that $A_{coh} \approx \lambda^2 R^2 / A'$, where λ is the wavelength of the light, R is the distance from Ω_i to the detector, and A' is the apparent area of Ω_i as seen by the detector. An additional factor A_{coh}/A_{det} is introduced into the relative spectrum of the interference terms. Since each A_{coh} may be considered as fluctuating independently, the relative spectrum is reduced by the number of these independent areas A_{det}/A_{coh}. $S_N(f)$, however, is unaffected since it is not an interference effect. The relative intensity spectrum then becomes

$$\frac{S_I(f)}{\bar{I}^2} = \frac{8DK^2 A_{coh}/A_{det}}{4D^2K^4 + (2\pi f)^2} + \frac{4D}{n_0 \Omega_i^2} \int \frac{|B_q|^2 q^2 \, d^3\boldsymbol{q}}{D^2 q^4 + (2\pi f)^2}. \tag{8}$$

The position of the halfwidth of the Lorentzian, $f_{1/2} = DK^2/\pi$, allows one to determine the diffusion constant, D. The low frequency limit of the Lorentzian, $2A_{coh}/A_{det}DK^2 = 2A_{coh}/\pi f_{1/2} A_{det}$, then allows one to determine A_{coh} if A_{det} is known. The Lorentzian is expected to be on top of a 'background' spectrum due to number fluctuations. For small enough Ω_i or n_0, the number fluctuations may dominate the Lorentzian. The high frequency limit of the relative number fluctuations from equation (6)

$$S_I(f)/\bar{I}^2 \to D^{1/2} A / 2n_0 \Omega_i^2 \pi^{3/2} f^{3/2} \qquad (f \gg f_3) \tag{9}$$

allows one to determine n_0 if D, A and Ω_i are known.

3. Experiment

In our experiment, light from a helium–neon laser ($\lambda = 6328$ Å) with a beam diameter of 1·7 mm passed through a small aperture of diameter 0·45 mm, and was focused by a microscope objective lens on to a thin closed cell containing a suspension of polystyrene

spheres in distilled water. Light scattered through an angle θ passed through an aperture of area A_{det} at a distance R from the cell and was incident on a photomultiplier 3 cm behind the aperture. The cell windows were carefully cleaned to minimize stray light that would generate a heterodyne component. We estimate that the heterodyne contribution to the Lorentzian was at most 5%. The photomultiplier output was amplified, digitized at a rate f_0 (points s^{-1}), and interfaced to a PDP-11 computer. The computer used a fast Fourier transform algorithm to measure the fluctuation spectrum in the range $f_0/1024$ to $f_0/2$. By taking successive runs with different values of f_0, we were able to determine the spectrum from 5×10^{-4} Hz to 5×10^{3} Hz. The high frequency limit was set by the digitizing electronics while the low frequency limit was set by the experimenters' patience, and possible settling effects of the particles. Each spectrum was averaged over at least 30 times the longest period. Thus, for example, the time taken to obtain a spectrum whose lowest frequency was 5×10^{-4} Hz was about 17 h.

Our arrangement of passing the laser light through an aperture and focusing it on to the sample cell produced an illuminated cylindrical volume, Ω_i, of length $l_0 = 1{\cdot}5$ mm with sharp boundaries and illumination uniform to within 10%. The diameter of the cylinder d could be varied by changing the beam focus. The minimum beam diameter was 10 ± 2 μm. Since the particles could not cross the ends of the cylinder, we expect the shape of the number fluctuation spectrum, $S_N(f)$, to be given by equation (4) with $f_1 \to 0$, and $f_2 = f_3 \approx D/\pi d^2$. Thus, $S_N(f)$ should be proportional to $f^{-3/2}$ for $f \gtrsim D/\pi d^2$, and flatten as f is lowered below $D/\pi d^2$. From equation (9) for a cylindrical Ω_i the high frequency limit of the number fluctuation contribution is

$$S_I(f)/\bar{I}^2 \to 8D^{1/2}/\pi^{5/2} n_0 d^3 l_0 f^{3/2} \qquad (f \gg f_3). \tag{10}$$

Figure 1 shows $S_I(f)/\bar{I}^2$ for a homodyne experiment on spheres of radius $r_0 = 630$ Å with $\theta = 50°$, $d = 10$ μm, $R = 4$ cm, and $n_0 \approx 5\times10^{11}$ cm^{-3}. The value of n_0 was

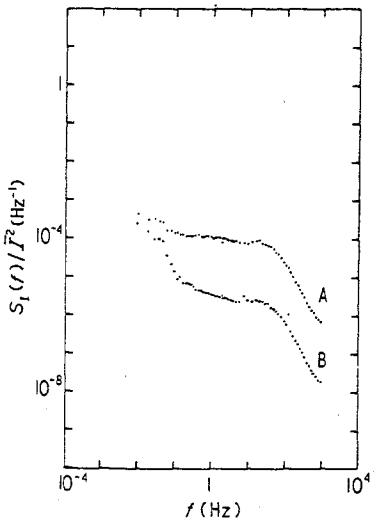

Figure 1. Effect of changing A_{det} on $S_I(f)/\bar{I}^2$ for light scattered from a suspension of polystyrene spheres with $r_0 = 630$ Å, $\theta = 50°$, $d = 10$ μm, $R = 4$ cm and $n_0 \approx 5\times10^{11}$ cm^{-3} A, $A_{det} = 0{\cdot}009$ cm^2; B, $A_{det} = 0{\cdot}7$ cm^2.

estimated from information supplied by the manufacturer† of the polystyrene spheres and our known dilution. Because of settling of the particles and evaporation of the solvent, the value of n_0 is accurate only to within a factor of 2. In figure 1 (curve A), $A_{det} = 0{\cdot}009\ \text{cm}^2$, and the spectrum is the usual homodyne Lorentzian. From the position of the halfwidth, $f_{1/2} = DK^2/\pi$, we may measure D. Here $K = 4\pi n \sin(\theta'/2)/\lambda$, where n is the index of refraction of the solvent, λ is the vacuum wavelength of the light, and θ' is the angle through which the light is scattered in the suspension. Using Snell's law to correct for refraction at the water–glass–air interface, we find that $\theta = 50°$ corresponds to $\theta' = 37{\cdot}2°$ inside the cell. Using the value of $f_{1/2} = 85$ Hz from figure 1 (curve A), we find $D = 4{\cdot}2 \times 10^{-8}\ \text{cm}^2\ \text{s}^{-1}$. This is in reasonable agreement with the value of $D = 3{\cdot}73 \times 10^{-8}\ \text{cm}^2\ \text{s}^{-1}$ calculated from the Einstein–Stokes relation (Einstein 1956) $D = k_B T/6\pi\eta r_0$, at room temperature. The major error in the measurement of D probably arose from the uncertainty in our estimate of θ.

In figure 1 (curve B), A_{det} was increased by a factor of 77 to $0{\cdot}7\ \text{cm}^2$. The low frequency limit of the Lorentzian was reduced by a factor of 65, demonstrating the effect of A_{coh}/A_{det} in determining the absolute magnitude of the homodyne interference spectrum. From the low frequency limit, we find $2A_{coh}/A_{det}DK^2 = 1{\cdot}7 \times 10^{-6}\ \text{Hz}^{-1}$, and estimate $A_{coh} = 1{\cdot}6 \times 10^{-4}\ \text{cm}^2$ at the aperture. The empirical formula $A_{coh} \approx \lambda^2 R^2/A'$ yields a value of $7{\cdot}0 \times 10^{-4}\ \text{cm}^2$. ($A'$ was corrected for the effect of the water–glass–air interface.) The number fluctuation contribution is unaffected by the change in A_{det} and therefore becomes more apparent at the low frequency end of the spectrum in figure 1 (curve B).

Figure 2 shows the effect of changing particle concentration for a given experimental configuration with $r_0 = 630$ Å, $\theta = 50°$, $d = 10\ \mu\text{m}$, and $A_{det} = 0{\cdot}7\ \text{cm}^2$. R was reduced to 3 cm in order to make the number fluctuations more apparent by decreasing A_{coh} and further suppressing the Lorentzian below that in figure 1 (curve B). For a

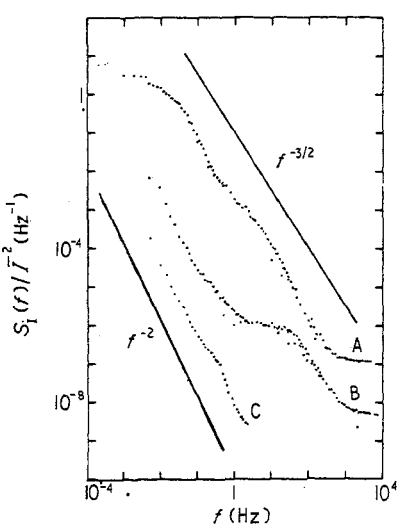

Figure 2. Effect of changing n_0 on $S_I(f)/\bar{I}^2$ with $r_0 = 630$ Å, $\theta = 50°$, $d = 10\ \mu\text{m}$, $A_{det} = 0{\cdot}7\ \text{cm}^2$, and $R = 3$ cm. A, $n_0 \approx 10^9\ \text{cm}^{-3}$ and $\langle N \rangle = 77$; B, $n_0 \approx 5 \times 10^{11}\ \text{cm}^{-3}$ and $\langle N \rangle = 5{\cdot}5 \times 10^4$; C, laser intensity fluctuation spectrum.

† Dow Chemical Company.

given value of Ω_i, we see from equation (8) that the relative interference fluctuations are independent of n_0 while the number fluctuations are proportional to n_0^{-1}. In figure 2 (curve B), n_0 is estimated to be 5×10^{11} cm^{-3}. At the lower frequencies, the $f^{-3/2}$ number fluctuation spectrum becomes apparent. In figure 2 (curve A), the suspension was diluted by a factor of 500 to give an estimated n_0 of 10^9 cm^{-3}. The number fluctuations are observed to increase by a factor of about 750 to dominate the Lorentzian. A shoulder due to the Lorentzian is, however, still visible above 1 Hz. As predicted by equation (4), as the frequency is lowered, there is an eventual flattening of the spectrum. The frequency below which this is expected, $D/\pi d^2 = 1{\cdot}3\times10^{-2}$ Hz, is in excellent agreement with experiment. As noted above, if D is known (say from the Lorentzian halfwidth), the absolute magnitude of the high frequency behaviour of the number fluctuations can be used to measure n_0. Using our measured value of $D = 4{\cdot}2\times10^{-8}$ cm^2 s^{-1} and equation (10), we find that, for figure 2 (curve A), $S_I(f)/\bar{I}^2 = 1{\cdot}0\times10^{-3}$ Hz^{-1} at 1·0 Hz and $n_m = 6{\cdot}6\times10^8$ cm^{-3}, where n_m is the *measured* concentration. In figure 2 (curve B), $S_I(f)/\bar{I}^2 = 1{\cdot}3\times10^{-6}$ Hz^{-1} at 1·0 Hz and from equation (10), we find $n_m = 4{\cdot}7\times10^{11}$ cm^{-3}. Both of these values are within the limits of our estimated n_0. The flattening of the spectra in figure 2 (curves A and B) above 1 kHz is due to shot noise in the photomultiplier. Using our measured values of n_m, we find that in figure 2 curve A has $\langle N\rangle = 77$, while curve B has $\langle N\rangle = 5{\cdot}5\times10^4$.

For comparison, curve C shows the relative intensity spectrum for the laser used, measured by replacing the sample cell by ground glass. The laser was not stabilized and the fluctuations were due primarily to a drift in the output intensity. Such a monotonic drift gives an f^{-2} spectrum with our measurement technique. The laser intensity fluctuations were orders of magnitude below the number and interference fluctuations. With an intensity stabilized laser it should be possible to see number fluctuations with $\langle N\rangle$ much greater than 10^5.

Figure 3 shows the effect of changing Ω_i, with $r_0 = 630$ Å, $\theta = 50°$, $A_{det} = 0{\cdot}7$ cm^2, $R = 3$ cm, and n_0 estimated to be 10^9 cm^{-3}. Figure 3 (curve A) reproduces figure 2 (curve A) with $d = 10$ μm. In figure 3 (curve B) the beam was defocused to give a larger Ω_i. In addition to decreasing the relative number fluctuations and moving the knee to a lower frequency, the increase in Ω_i reduces A_{coh} and suppresses the Lorentzian. The spectrum is close to $f^{-3/2}$ over five decades while no definite knee or Lorentzian is apparent. Again, the high frequency flattening is due to photomultiplier shot noise. Although we could not make a direct measurement, the value of d in figure 3 (curve B) can be determined from equation (10) and the ratio of the $f^{-3/2}$ regions in figure 3 (curves A and B). We find $d = 120$ μm and predict that the knee should occur at $D/\pi d^2 = 9\times10^{-5}$ Hz, which is below the lowest frequency measured. In figure 3 (curve B) $\langle N\rangle = 1{\cdot}1\times10^4$.

We performed a similar set of experiments on larger spheres, with $r_0 = 6500$ Å, $\theta = 30°$, $A_{det} = 0{\cdot}7$ cm^2, and $R = 6$ cm. With a large scattering volume and a relatively high particle concentration we observed the expected interference Lorentzian. The halfwidth was 2 Hz, corresponding to $D = 2{\cdot}5\times10^9$ cm^2 s^{-1}. The spectrum for $d = 10$ μm and $n_m = 4{\cdot}7\times10^7$ cm^{-3} is shown in figure 3 (curve C). The knee of the Lorentzian is still just visible; below the knee frequency, the $f^{-3/2}$ behaviour due to number fluctuations is observed. The spectrum is expected to begin to flatten off at frequencies below $D/\pi d^2 = 8\times10^{-4}$ Hz. Although the lowest few points of figure 3 (curve C) show some degree of flattening that may be the start of this knee, the lowest points are unreliable because of a noticeable settling of the larger spheres over the 16 h time span of the experiment.

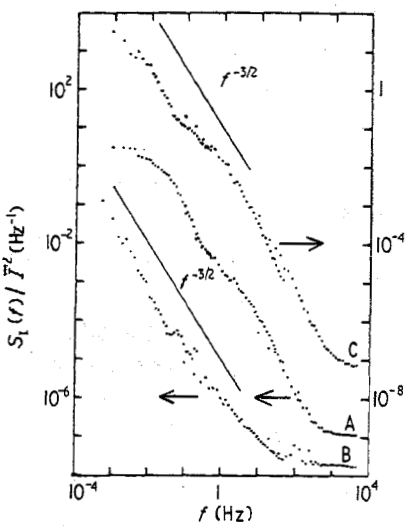

Figure 3. (Left-hand scale) effect of changing Ω_i on $S_I(f)/\bar{I}^2$ with $r_0 = 630$ Å, $\theta = 50°$, $A_{det} = 0{\cdot}7$ cm^2, $R = 3$ cm, $n_0 \approx 10^9$ cm^{-3}. A, $d = 10$ μm (reproduces figure 2 (curve A)); B, $d \approx 120$ μm. C (right-hand scale), measured $S_I(f)\ \bar{I}^2$ for larger spheres with $r_0 = 6500$ Å, $\theta = 30°$, $A_{det} = 0{\cdot}7$ cm^2, $R = 6$ cm.

In the forward direction the approximation $|\boldsymbol{K}| \gg 1/l$ breaks down. As the main beam is detected by the photomultiplier, the heterodyne fluctuations dominate the spectrum. Figure 4 (curve A) shows the spectrum from an experiment in the forward direction in which the main beam is detected, with $r_0 = 630$ Å, $\theta = 0°$, $A_{det} = 0{\cdot}7$ cm^2, $R = 10$ cm, and n_0 estimated to be 5×10^{11} cm^{-3}. If one assumes that $\boldsymbol{K}$ is exactly zero in the forward direction, there is no first order phase change when a particle moves, and we see from equation (2) that the interference terms have no finite frequency contribution. One would then expect to observe only number fluctuations and a spectrum like figure 2 (curve A). Although the spectrum of figure 4 (curve A), has a knee at 10^{-2} Hz, it is much sharper than the knee in figure 2 (curve A), and the behaviour between 10^{-2} Hz and 10 Hz is steeper than $f^{-3/2}$. We conclude that the fluctuations are due to heterodyne interference with a distribution of small $\boldsymbol{K}$ values. From the position of the knee at 10^{-2} Hz, we estimate that $|\boldsymbol{K}| < 10^3$ cm^{-1}. A rough estimate of the range of θ's included due to the finite A_{det} gives $|\boldsymbol{K}| < 4 \times 10^3$ cm^{-1}.

The number fluctuations are not an interference effect. It should, therefore, be possible to observe the number fluctuation spectrum with white or incoherent light. Figure 4 (curves B, C and D) shows the spectra obtained from several experiments in which the light source was a DC powered incandescent bulb. In curve B, $r_0 = 6500$ Å, $\theta = 45°$, $A_{det} = 0{\cdot}7$ cm^2, n_0 is estimated to be 5×10^8 cm^{-3} and $R \approx 1$ cm. Ω_i was determined by a slit 130 μm × 10 μm immediately in front of the sample cell rather than by a focused beam. Although the photomultiplier shot noise is more apparent, there is no interference Lorentzian and the $f^{-3/2}$ number fluctuation spectrum is quite clear. Using equation (9), and our measured $D = 2{\cdot}5 \times 10^{-9}$ cm^2 s^{-1}, we determine $n_m = 2{\cdot}3 \times 10^9$ cm^{-3} from the magnitude of the $f^{-3/2}$ region. In curve C, $r_0 = 630$ Å, $\theta = 50°$, $A_{det} = 0{\cdot}7$ cm^2, $n_0 \approx 2 \times 10^{11}$ cm^{-3}, and $R = 6$ cm. The microscope objective lens was used to focus an image of the bulb filament in the cell, and so produce an Ω_i of

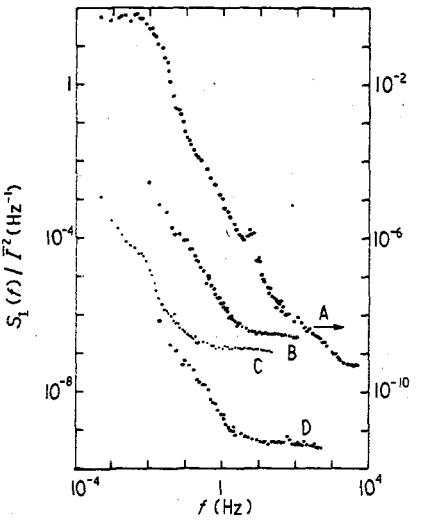

Figure 4. A (right-hand scale), measured $S_I(f)/\bar{I}^2$ for laser light scattered in the forward direction with $r_0 = 630$ Å, $\theta = 0°$, $A_{det} = 0{\cdot}7$ cm^2, $R = 10$ cm, and $n_0 \approx 5\times10^{11}$. B, C and D (left-hand scale), $S_I(f)/\bar{I}^2$ observed with a white light source: B, $r_0 = 6500$ Å, $\theta = 45°$, $A_{det} = 0{\cdot}7$ cm^2, $n_0 \approx 5\times10^8$ cm^{-3}, $R \approx 1$ cm, Ω_i determined by a slit 130 μm × 10 μm and $\langle N\rangle = 5\times10^3$; C, $r_0 = 630$ Å, $\theta = 50°$, $A_{det} = 0{\cdot}7$ cm^2, $R = 6$ cm, and $n_0 \approx 2\times10^{11}$ cm^{-3}, and Ω_i determined by a focused image of the filament; D, $r_0 = 630$ Å, $\theta = 0°$, $A_{det} = 0{\cdot}7$ cm^2, $R \approx 1$ cm, $n_0 \approx 2\times10^{11}$ cm^{-3}, Ω_i determined by a slit 20 μm × 2 mm, and $\langle N\rangle = 8\times10^6$.

irregular shape for which no numerical calculations could be made. However, as expected, the spectrum is still proportional to $f^{-3/2}$ since the dimensions of Ω_i were greater than $(D/f)^{1/2}$. In curve D, $r_0 = 630$ Å, $\theta = 0°$, $A_{det} = 0{\cdot}7$ cm^2, $n_0 \approx 2\times10^{11}$ cm^{-3}, and $R \approx 1$ cm. Ω_i was again determined by a slit of dimensions 2 mm × 20 μm immediately in front of the cell. Although the $f^{-3/2}$ behaviour is apparent, its magnitude cannot in general be used to determine n_m from equation (9) as it was in figure 4 (curve B). Since we are observing the main beam, $\bar{I} \neq \langle N\rangle\beta^2$. It is, however, sufficient to adopt a simple model in which $I = I_0 \exp(-N\sigma/a)$, where I is the transmitted intensity, I_0 is the incident intensity, N is the number of particles in the beam, σ is the cross section for scattering out of the beam, and a is the beam area. In this case, $S_I(f)/\bar{I}^2 = [\ln(I_0/I)]^2 S_N(f)/\langle N\rangle^2$, and the spectrum must be scaled by $[\ln(I_0/I)]^2$. Here, $I_0/I \approx 2$, and we find $n_m = 1{\cdot}2\times10^{11}$ cm^{-3}. In figure 4 (curve D), $\langle N\rangle = 8\times10^6$. The increased intensity stability of the bulb over the laser and the absence of interference fluctuations allow one to easily observe the number fluctuations, even when $\langle N\rangle > 10^6$

4. Discussion

We have shown experimentally that $S_I(f)/\bar{I}^2$ contains a number fluctuation term, $S_N(f)/\bar{N}^2$, in addition to the usual interference terms. The determination of $S_N(f)/\bar{N}^2$ provides information about n_0 and also about the shape of the scattering volume Ω_i.

In previous measurements of intensity fluctuations the autocorrelation function was invariably measured, presumably because of the availability of fast commercial correlators. The use of the fast Fourier transform, however, gives a direct spectral

measurement the same multiplexing advantage with fewer computations. Although the power spectrum and the autocrorrelation function are formally equivalent via the Wiener–Khintchine relations, because each is measured over a limited range it is often impossible to calculate one from the other without introducing errors. Thus, for different applications, a direct measurement of either the power spectrum or the autocorrelation function may be preferable. For example, although n_0 may be measured either from $\langle \delta N(0)\, \delta N(\tau)\rangle$ as $\tau \to 0$ or from $S_N(f)$ as $f \to \infty$, the latter method may offer experimental advantages. Other noise sources contribute to $\langle \delta N(0)\, \delta N(0)\rangle$ and may make it difficult to identify the contribution of the number fluctuations. On the other hand, the $f^{-3/2}$ dependence of $S_N(f)$ at high frequencies offers an unmistakable signature of number fluctuations, even when $\bar{N}$ is as high as 10^6. Moreover, $S_N(f)$, rather than the autocorrelation function, reflects the shape of Ω_i in a straightforward way.

5. Acknowledgments

We wish to thank Dr M P Klein and Dr M Kronick for helpful discussions. Dr Klein kindly supplied the polystyrene spheres. This work was supported by the USERDA.

Appendix

We wish to calculate the positive frequency spectrum of the intensity fluctuations, which is given by the cosine transform of the autocorrelation function

$$S_I(f) = 4\int_0^\infty \langle I(0)I(\tau)\rangle \cos(2\pi f\tau)\, d\tau.$$

The calculation of $\langle I(0)I(\tau)\rangle$ involves the average of the product of four terms similar to equation (1), two at $t = 0$, and two at $t = \tau$. Because of our assumption that $B_K = 0$, cross terms of the form $\langle B(\boldsymbol{r}) \cos(\boldsymbol{K}\cdot\boldsymbol{r})\rangle$ vanish. Since each particle is independent, terms containing more than one index factor into the product of averages for each index. Thus, for example,

$$\langle B(\boldsymbol{r}_j)B(\boldsymbol{r}_k)\, e^{i\boldsymbol{K}\cdot(\boldsymbol{r}_j-\boldsymbol{r}_k)}\rangle = \langle B(\boldsymbol{r}_j)\, e^{i\boldsymbol{K}\cdot\boldsymbol{r}_j}\rangle\langle B(\boldsymbol{r}_k)\, e^{-i\boldsymbol{K}\cdot\boldsymbol{r}_k}\rangle = \begin{cases} 0 & \text{for } j \neq k, \\ \langle B\rangle = \Omega_i/\Omega & \text{for } j = k. \end{cases}$$

Hence

$$\langle I(0)I(\tau)\rangle = E_0^4 + 2\beta^2 E_0^2\langle N\rangle + 4(\boldsymbol{\beta}\cdot\boldsymbol{E}_0)^2 \sum_{jl} \langle B(\boldsymbol{r}_j)B(\boldsymbol{r}_l)\cos(\boldsymbol{K}\cdot\boldsymbol{r}_j)\cos(\boldsymbol{K}\cdot\boldsymbol{r}_l)\rangle + \beta^4 \sum_{jklm} \langle B(\boldsymbol{r}_j)B(\boldsymbol{r}_k)B(\boldsymbol{r}_l)B(\boldsymbol{r}_m)\, e^{i\boldsymbol{K}\cdot(\boldsymbol{r}_j-\boldsymbol{r}_k)}\, e^{i\boldsymbol{K}\cdot(\boldsymbol{r}_l-\boldsymbol{r}_m)}\rangle, \tag{A.1}$$

where $\langle N\rangle = M\Omega_i/\Omega$. The indices j and k refer to $t = 0$, while l and m refer to $t = \tau$. The third term in equation (A.1) is non-zero only for $j = l$, while the fourth term is non-zero only when each index is equal to at least one other index. After some manipulation, equation (A.1) can be put in the form, for $M \gg 1$:

$$\langle I(0)I(\tau)\rangle = E_0^4 + 2\beta^2 E_0^2\langle N\rangle + 2(\boldsymbol{\beta}\cdot\boldsymbol{E}_0)^2 M(F_+(\boldsymbol{K},\tau) + F_-(\boldsymbol{K},\tau)) + \beta^4 M F_-(0,\tau) + \beta^4\langle N\rangle^2 + \beta^4 M^2(F_+^2(\boldsymbol{K},\tau) + F_-^2(\boldsymbol{K},\tau)) \tag{A.2}$$

where

$$F_{\pm}(\boldsymbol{K}, \tau) = \Omega^{-1} \int_{\Omega} d^3\boldsymbol{r} \int_{\Omega} d^3\boldsymbol{r}' B(\boldsymbol{r}) B(\boldsymbol{r}') \, e^{i\boldsymbol{K}\cdot(\boldsymbol{r}\pm\boldsymbol{r}')} P(\boldsymbol{r}, 0 | \boldsymbol{r}', \tau). \tag{A.3}$$

$P(\boldsymbol{r}, 0|\boldsymbol{r}', \tau)\, d^3\boldsymbol{r}'$ is the probability that a particle at $\boldsymbol{r}$ at $t = 0$ will be in $d^3\boldsymbol{r}'$ about $\boldsymbol{r}'$ at $t = \tau$, and in the usual diffusion approximation (Chandrasekhar 1943) is given by

$$P(\boldsymbol{r}, 0 | \boldsymbol{r}', \tau) = (4\pi D\tau)^{-3/2} \exp[-(\boldsymbol{r}' - \boldsymbol{r})^2 / 4D\tau]. \tag{A.4}$$

It remains to evaluate $F_{\pm}(\boldsymbol{K}, \tau)$. By introducing $\boldsymbol{s} = \boldsymbol{r}' - \boldsymbol{r}$ in equation (A.3), and taking spatial transforms, we find

$$F_{\pm}(\boldsymbol{K}, \tau) = \Omega^{-1} \int d^3\boldsymbol{q} B_{-\boldsymbol{q}} B_{\boldsymbol{q}+\boldsymbol{K}\pm\boldsymbol{K}} \, e^{-D(K+q)^2\tau}. \tag{A.5}$$

Using the approximation $B_{\boldsymbol{K}} = 0$, we use equation (A.5) in equation (A.2) to find

$$\langle I(0) I(\tau) \rangle = \text{constant} + 2(\boldsymbol{\beta} \cdot \boldsymbol{E}_0)^2 \langle N \rangle \, e^{-DK^2\tau} + \beta^4 \langle N \rangle^2 \, e^{-2DK^2\tau} + \beta^4 \langle \delta N(0) \, \delta N(\tau) \rangle \tag{A.6}$$

where $\langle \delta N(0) \, \delta N(\tau) \rangle = MF_{-}(0, \tau)$ is the autocorrelation function for number fluctuations in Ω_i due to diffusion of the particles. $F_{-}(0, \tau)$ is the probability that a particle in Ω_i at $t = 0$ will also be in Ω_i at $t = \tau$. $1 - F_{-}(0, \tau)$ is the probability after-effect factor of Chandrasekhar (1943).

The cosine transform of equation (A.6) gives the frequency spectrum. Apart from zero-frequency components, we find

$$S_I(f) = \frac{8(\boldsymbol{\beta} \cdot \boldsymbol{E}_0)^2 \langle N \rangle DK^2}{D^2K^4 + (2\pi f)^2} + \frac{8\beta^4 \langle N \rangle^2 DK^2}{4D^2K^4 + (2\pi f)^2} + \beta^4 S_N(f) \tag{A.7}$$

where $S_N(f)$ is given by equation (3). The first and second terms are the heterodyne and homodyne Lorentzians (Cummins and Swinney 1970). The heterodyne term vanishes as $\boldsymbol{E}_0 \to 0$, and by dividing the remaining terms of equation (A.7) by $\bar{I} = \beta^2 \langle N \rangle$, we obtain equation (2).

References

Chandrasekhar S 1943 *Rev. Mod. Phys.* **15** 1–89

Cummins H Z, Knahle N and Yeh Y 1964 *Phys. Rev. Lett.* **12** 150–3

Cummins H Z and Swinney H L 1970 *Progress in Optics* vol 8, ed E Wolf (Amsterdam, London: North-Holland) pp 133–200

Einstein A 1956 *Investigations on the Theory of Brownian Movement* ed R Furth (New York: Dover)

Elson E L and Magde D 1974 *Biopolymers* **13** 1–19

Ford N C and Benedek G B 1965 *Phys. Rev. Lett.* **15** 649–53

Magde D, Elson E L and Webb W W 1974 *Biopolymers* **13** 20–62

Pusey P N, Schaefer D W and Koppel D E 1974 *J. Phys. A: Math., Nucl. Gen.* **7** 530–40

Schaefer D W, Banks G and Alpert S S 1974 *Nature* **248** 162–4

Schaefer D W and Berne B J 1972 *Phys. Rev. Lett.* **28** 475–8

Schaefer D W and Pusey P N 1972 *Phys. Rev. Lett.* **29** 843–5

van Vliet K M and Fasset J R 1965 *Fluctuation Phenomena in Solids* ed R E Burgess (New York: Academic) pp 267–354

van der Ziel A 1954 *Noise* (New York: Prentice-Hall) pp 438–43